Dynamic Modeling of Hydraulic Power Steering System with Variable Ratio Rack and Pinion Gear*

Nong ZHANG** and Miao WANG**

A comprehensive mathematical model of a typical hydraulic power steering system equipped with variable ratio rack and pinion gear is developed. The steering system's dynamic characteristics are investigated and its forced vibrations are compared with those obtained from a counterpart system with a constant ratio rack and pinion gear. The modeling details of the mechanism subsystem, hydraulic supply lines subsystem and the rotary spool valve subsystem are provided and included in the integrated steering system model. The numerical simulations are conducted to investigate the dynamics of the nonlinear parametric steering system. From the comparison between simulated results and the experimental ones, it is shown that the model accurately integrates the boost characteristics of the rotary spool valve which is the key component of hydraulic power steering system. The variable ratio rack-pinion gear behaviors significantly differently from its constant ratio counterpart does. It significantly affects not only the system natural frequencies but also reduces vibrations under constant rate and ramp torque steering inputs. The developed steering model produces valid predictions of the system's behavior and therfore could assist engineers in the design and analysis of integrated steering systems.

Key Words: Dynamic Modeling, Hydraulic Power Steering, Variable Ratio Rack and Pinion Steering Gear

1. Introduction

The steering system equipped with rack and pinion gear is widely used in automotives due to its advantages, such as higher mechanical efficiency and fewer linkage parts. The variable ratio (VR) rack and pinion steering mechanism was invented and improved to enhance the vehicle on-center handling performance and reduce the lock-to-lock circles of the steering wheel. The variable ratio of a rack and pinion gear is usually achieved by the continuously variable shapes of the teeth of the rack from the center to the two ends. Figure 1 shows the ratio characteristics of a typical variable ratio rack and pinion steering gear. The rack gain (deg/mm) in the center range of the rack is much higher than the rack gain at the two ends of the rack. This means that the pinion needs to have more angular displacement in the center of rack than that it needs to have at the two ends of the rack to push the rack with the same distances, and in another word, the steering ratio (rotating degree of steering wheel/rotating degree of the front wheels) in the center of the rack is greater that the ratio at the two ends of the rack.

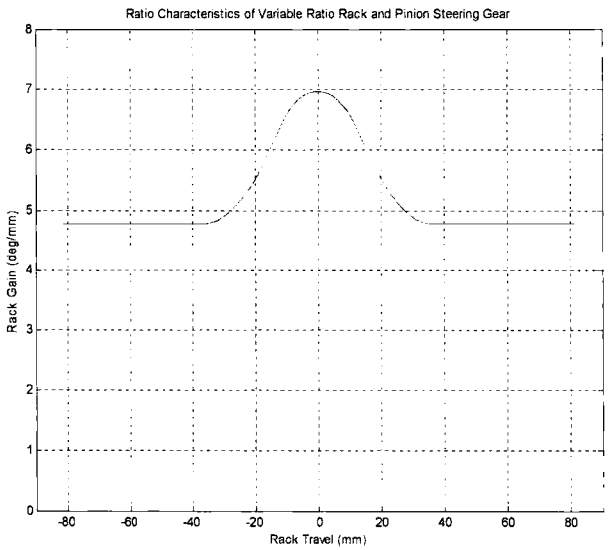

Fig. 1 Ratio characteristics of variable ratio rack and pinion steering gear

* Received 4th January, 2005 (No. 05-5001)

** Faculty of Engineering, University of Technology Sydney, PO Box 123, Broadway, NSW 2007, Australia.
E-mail: nong.zhang@uts.edu.au

Most modern vehicles have power assistant steering systems to increase the handling performance of vehicles and reduce the input torque on the steering wheel, because the manual torque required to turn the wheels gets higher as the front axle load of the vehicle gets higher. Hydraulic power steering systems are playing a main role in steering assistance on the market because of their higher assistant force, higher reliability and lower cost. While hydraulic power steering system has many advantages, vibration and noise phenomena[1] exist in the system and need to be solved properly.

Steering system mathematical models are efficient tools and are widely used to analyse and improve the performance of steering systems. A number of models of no assistant power rack and pinion gear steering systems have been developed by researchers. A steering model with free-play and dry friction[2] was used in the vehicle dynamics simulation. Steering system parameters were analysed and optimized in a steering system model[3] with front suspensions. Bond Graph technique was adopted by Vijayakumar and Barak[4] to simulate steering systems. Sharp and Granger[5] developed a model to investigate the main influences of steering torque at parking speeds. However, these developed models are not suitable for describing the dynamics of power steering systems which are much more complicated than the no assistant power systems.

In order to investigate hydraulic power steering system dynamics, Ferries and Arbanas[6] constructed the system as a feedback control system, and studied it in the frequency domain by using control theory. Simplified valve and hydraulic supply line mathematic models were introduced in the investigation on self-excited vibration[7]. Qatu, el al.[8]-[10] took much concern with the hydraulic circuit dynamics, whereas Phillips[11] developed a coupled mathematical model focusing on the vibration of the hydraulic actuator. Steering wheel nibbles, the rotational vibrations of the steering wheels, were investigated in the research described in paper[12] where models of suspension and steering systems were developed and the sensitivities of suspension and steering parameters were also analysed. Takeuchi and Adachi[13] used characteristic matrices to study the noise of hydraulic power steering systems in frequency domain. A steering system model[14] with simplified hydraulic boost force function was developed to simulate the effects of steering system on vehicle on-center handling. Sensitivity of key parameters of the hydraulic power steering system is investigated[19], including the shapes of the valve edges and the fluctuations of pump flow rate and pressure.

While the previous steering models had different emphases and advantages, an integrated model of hydraulic power steering system, which includes the detailed dynamic characteristics of the hydraulic line, the valve and the mechanism, still need to be developed for the accurate vibration analysis of the system. Also, it is found that none of the foregoing models includes the variable ratio rack and pinion gear set. Though the effects of the VR steering system on vehicle dynamics have been convincingly discussed by Heathershaw[15],[16], the steady state and transient dynamic characteristics of the hydraulic power variable ratio steering system itself has not been seriously investigated and reported.

Focusing on the interconnections of different components and the transient dynamic responses of the complete system with the variable ratio rack and pinion gear, a non-linear model of hydraulic power steering system is proposed in this paper. In the model, mechanical parts of the system are developed as lumped masses interconnected with springs and dampers. By integrating the cylinder, pump and hoses, a hydraulic circuit model is obtained where these hydraulic elements are constructed as hydraulic impedance elements, and the rotary spool valve, the key component of the system, is modeled as a four-way open centre spool valve.

Based on the proposed mathematic model, free and forced vibration analyses are conducted to investigate dynamic behavior of the hydraulic power VR rack and pinion steering system. The dynamic characteristics of the VR system are compared with that of a constant ratio (CR) steering system with the same hydraulic circuits except the rack-pinion gear set. It is found that the natural frequencies and the dynamic responses of the VR steering system are different from those of the steering system with a constant ratio.

2. Mechanism Subsystem Model with Variable Ratio Rack and Pinion Gear

The dynamic components of a typical hydraulic power steering system mainly include steering wheel, input shaft, rotary spool valve, rack and pinion, pump, hydraulic cylinder, hydraulic hoses, tie rod linkage, front wheels and tyres. During a steering process, the rotational displacement between the sleeve and spool of the rotary spool valve caused by the driver steer input directs the hydraulic force to one side of the piston in the hydraulic cylinder. Since the piston is directly connected with the rack, the hydraulic force on the piston helps the driver steer the two front wheels.

A schematic of a power steering system is shown in Fig. 2. Different principles, methods and techniques are applied to model the mechanism, the hydraulic supply line and the rotary spool valve subsystems because of their evidently different dynamic nature.

As shown in Fig. 2, the steering column and torsional bar are modeled as springs and dampers, and the stiffness of pinion meshed with rack and the stiffness of tie rods are taken account of as well. The twist angle of torsional bar

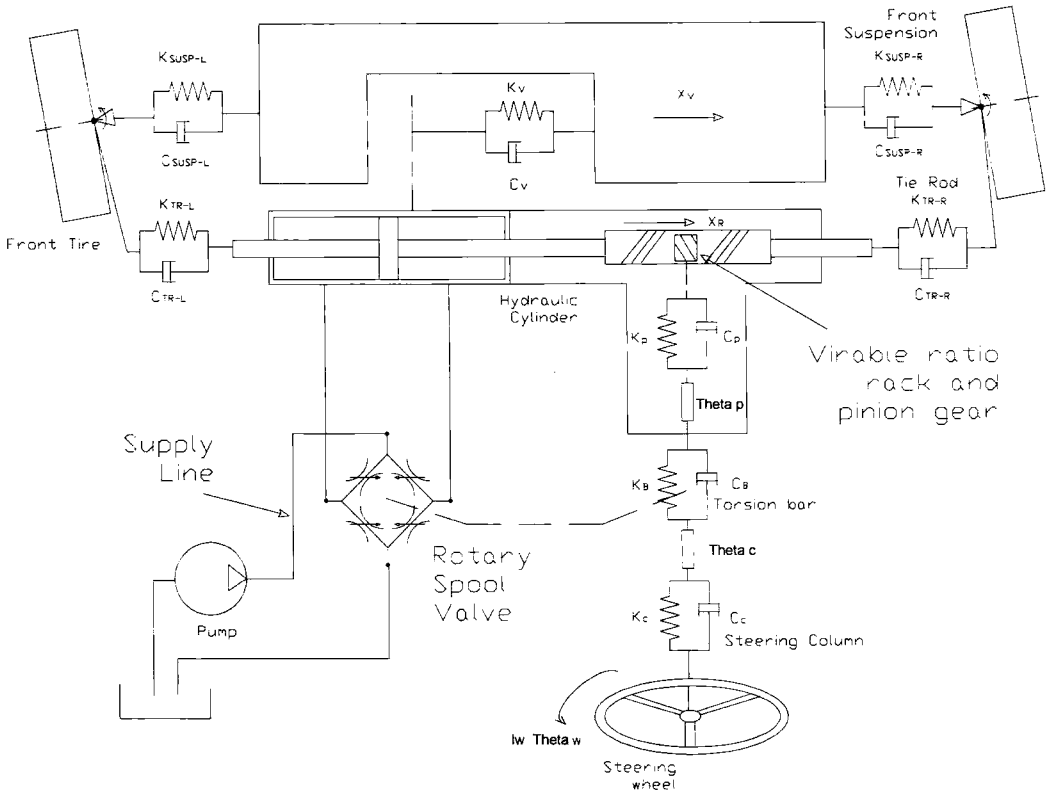

Fig. 2 Schematic of steering system model, including the connection with front suspensions

controls the spool valve and this is the key connection between mechanism subsystem and valve subsystem (shown in Fig. 2 as dash line). The lateral forces of tie rods produce the rotational torque and steer two front wheels by the steering arms. In this model, not only the rotational degrees of freedom of the front wheels are introduced but also the lateral movement of front wheels. The hydraulic cylinder is mounted on the vehicle body by spring and damper, therefore the interaction between the steering system and vehicle body is involved. The lateral displacement of the front part of the vehicle body transfers the vibration from hydraulic cylinder to the front wheels through the left and right front suspensions. A simplified tyre model is used, which includes both the torsional and lateral stiffness of the tyres.

Friction also greatly affects the dynamics of the system. The non-linear friction forces in this model include the friction on the steering column, the friction of the kingpins, the friction between rack and pinion, the friction between piston and hydraulic cylinder, and the friction between tyres and the ground. In the numerical analysis, the nonlinear friction forces are represented as hyperbolic tangent functions[5] to reduce the "stiffness" of the calculation. Since the steering vibration at parking speed is the main concern at this stage, the aligning torque on the tyres, which occurs in middle and high vehicle speed, is not involved.

A 12 degree of freedoms (DOFs) model shown in Eq. (1) represents the mechanism subsystem and it is formulated using free body diagrams and the Newton's Second law of motion. In the model, steering wheel, steering column, pinion, two front wheels and two tyres have the rotational DOFs (θ), and rack (with the piston and tie rods), hydraulic cylinder (housing), front vehicle body, two front wheels have linear displacements (x).

Corresponding to Fig. 2, θ_{SW} represents the angular displacement of steering wheel, θ_C is steering column, θ_P is the pinion, x_R is the rack, θ_{FW-L} and θ_{FW-R} are the left and right front wheels (road wheels) respectively, θ_{CP-L} and θ_{CP-R} are the angular displacements of the contact patches of the front tyres respectively, x_H is the hydraulic housing, x_V is the displacement of the front half of vehicle and x_{FW-L}, x_{FW-R} is the lateral displacement of the two front wheels. On the right hand side of Eq. (1), T and F represent the external torques and forces applied on the corresponding elements in the model.

The stiffness coefficient matrix of the complete steering system which is represented as $[K]_{12\times12}$ in Eq. (1) is given in the Appendix. The mechanical ratios are taken account of the ratio between rack and pinion and the ratio between the linear displacement of tie rods and the angular displacement of the steering arms. According to the lumped mass model shown in Fig. 2, it is evident that the damping matrix has the similar form to the stiffness matrix.

$$[M(I)]_{12\times12}[\ddot{\theta}(\ddot{x})]_{12\times1}+[C]_{12\times12}[\dot{\theta}(\dot{x})]_{12\times1}+[K]_{12\times12}[\theta(x)]_{12\times1}=[T(F)]_{12\times1} \quad (1)$$

Where

$$[\theta(x)]_{12\times1}=\begin{bmatrix}\theta_{SW}\\ \theta_C\\ \theta_P\\ x_H\\ x_R\\ \theta_{FW-L}\\ \theta_{FW-R}\\ \theta_{CP-L}\\ \theta_{CP-R}\\ x_{FW-L}\\ x_{FW-R}\\ x_V\end{bmatrix} \quad [T(F)]_{12\times1}=\begin{bmatrix}T_{SW}\\ -T_{FR-C}\\ -T_{FR-P}\\ F_{FR-H}-F_B\\ F_B-F_{FR-H}\\ -T_{FR-K}\\ -T_{FR-K}\\ -T_{FR-G}\\ -T_{FR-G}\\ 0\\ 0\\ 0\end{bmatrix}$$

Among the 12 second order coupled differential equations, Eq. (2) is the equation for the rack and it is explained here as an example. x_R, θ_P, θ_{FW-L}, and θ_{FW-R} are the independent coordinates of the rack (with piston and two tie rods), pinion, left and right front wheels respectively. C_P, K_P, C_{TR-L}, K_{TR-L}, C_{TR-R} and K_{TR-R} are the stiffness and damping of pinion, left and right tie rods. N is the gear ratio between rack and pinion, l is the distance from the end of tie rod to the center of tyre twisting, F_{FR-H} is the friction force between piston and hydraulic cylinder and F_B is the hydraulic boost force on piston. In the mechanism model, the boost force is determined by the spool valve model and is the main concern in the steering system vibration study.

$$\begin{aligned}&m_R\ddot{x}_R-\frac{C_P}{N}\dot{\theta}_P+\left(\frac{C_P}{N^2}+C_{TR-L}+C_{TR-R}\right)\dot{x}_R\\&-C_{TR-L}\cdot l\cdot\dot{\theta}_{FW-L}-C_{TR-R}\cdot l\cdot\dot{\theta}_{FW-R}\\&-\frac{K_P}{N}\theta_P+\left(\frac{K_P}{N^2}+K_{TR-L}+K_{TR-R}\right)x_R\\&-K_{TR-L}\cdot l\cdot\theta_{FW-L}-K_{TR-R}\cdot l\cdot\theta_{FW-R}=F_B-F_{FR-H}\end{aligned} \quad (2)$$

The characteristics of variable ratio rack and pinion gear set are included into the parametric system by changing the variable N in system matrices. Depending upon the positions of the rack and the rack gain curve shown in Fig. 1, value of N changes at every time step of the numerical simulation, and the mass matrix, stiffness matrix and damping matrix of the system are re-determined at every time step to obtain the system responses.

3. Hydraulic Supply Line Subsystem Model

Hydraulic power steering systems comprise a number of tubes and hoses connecting the pump, the valve and the reservoir. The low pressure return line of the steering system does not affect the system much so only the high pressure supply line is considered in this study.

Three main elements of a supply line are a steel tube connecting the pump, a tube connecting the spool valve, and a hose between them which is fabricated from wire braid and synthetic rubber. They are shown as Tube 1, Tube 2 and Hose respectively in Fig. 3. The modeling of the supply line takes into account the compressibility of the steering oil and the elasticity of hose and tubes which are essential parts for the hydraulic dynamics of the system.

Three main steps are used to develop the model of the supply line. At first, a tube or a hose is modeled as a single hydraulic element, and based on fluid impedance method[17], a lumped parameter model is applied to derive the impedance parameters. Then, a distributed parameter model[17] generates a dynamic relation of the inlet pressure, inlet flow rate, outlet pressure, and outlet flow rate. Finally, three transfer matrices of the three elements produce a total transfer matrix of the supply line and the dynamic relationships are obtained.

Figure 4 shows a lumped parameter model of one hydraulic tube/hose element. Because good analogies can be drawn between electrical circuits and hydraulic systems, electrical analogues are employed to analyse the hydraulic impedances.

Shown in Fig. 4, Q_u and P_u are the inlet flow rate and pressure, and the Q_d and P_d are the outlet ones. Fluid resistance, fluid inductance and fluid capacitance are represented by R_h, L_h and C_h respectively, and are listed in Eqs. (3),–(5),

$$R_h=\frac{128\mu L}{\pi d^4} \quad (3)$$

$$L_h=\frac{\rho L}{A} \quad (4)$$

$$C_h=\frac{AL}{\beta_e}, \quad (5)$$

where μ is the dynamic viscosity, L is the length of the tube or hose, d is the inner diameter of the tube or hose, ρ is the density of the fluid, A is the inner area of the pipe or hose, and β_e is the equivalent bulk modulus.

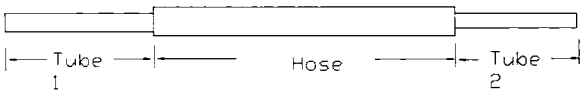

Fig. 3 Supply line

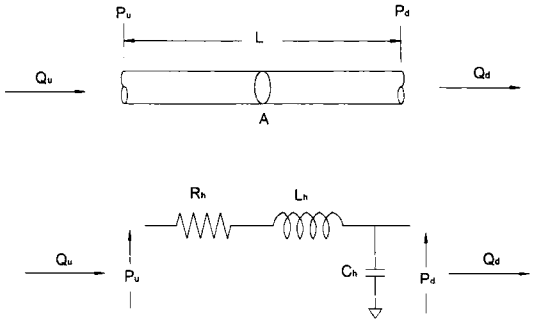

Fig. 4 A lumped parameter model of pipe line

Using the impedance parameters, the pressure oscillation and flow ripple are investigated by distributed parameter models. Every element of the supply line is described by a transfer matrix, like Eq. (6).

$$\begin{bmatrix} \hat{P}(l) \\ \hat{Q}(l) \end{bmatrix} = [T] \cdot \begin{bmatrix} \hat{P}(0) \\ \hat{Q}(0) \end{bmatrix} \tag{6}$$

where $\begin{bmatrix} \hat{P}(l) \\ \hat{Q}(l) \end{bmatrix}$ and $\begin{bmatrix} \hat{P}(0) \\ \hat{Q}(0) \end{bmatrix}$ are the outlet pressure, flow rate and the inlet pressure, flow rate respectively. The transfer matrix is

$$T = \begin{bmatrix} \cosh(rl) & -Z_c \sinh(rl) \\ \dfrac{\sinh(rl)}{Z_c} & \cosh(rl) \end{bmatrix}, \tag{7}$$

where $\gamma = \sqrt{C_h j\omega (L_h j\omega + R_h)}$ and $Z_c = \dfrac{\beta_e \gamma}{A \cdot j\omega}$.

For the supply line model, the outlet of tube 1 is the inlet of the hose, and the outlet of hose is the inlet of tube 2, therefore the transfer matrix of the whole supply line is obtained by multiplying three transfer matrices of the three elements.

$$T_{\sup} = T_{Tube-2} \cdot T_{Hose} \cdot T_{Tube-1} \tag{8}$$

The dynamic hydraulic responses of the supply line is shown in Eq. (9),

$$\begin{bmatrix} \hat{P}_S \\ \hat{Q}_S \end{bmatrix} = [T_{\sup}] \cdot \begin{bmatrix} \hat{P}_{pump} \\ \hat{Q}_{pump} \end{bmatrix} \tag{9}$$

Where $\begin{bmatrix} \hat{P}_{pump} \\ \hat{Q}_{pump} \end{bmatrix}$ and $\begin{bmatrix} \hat{P}_S \\ \hat{Q}_S \end{bmatrix}$ are the pressure, flow rate of the pump and the pressure, flow rate of the inlet of spool valve respectively. The output of supply line model supplies the dynamic input of rotary spool valve subsystem.

4. Rotary Spool Valve Subsystem Model

A typical rotary spool valve used in hydraulic power steering system can be modeled as a four-way open center valve which is shown in Fig. 5. Classical flow orifice equations, Eq. (10), describe the flow rate and pressure relations.

$$q_i = C_d A_i \sqrt{\frac{2}{\rho} |\Delta P_i|} \quad i = 1,2,3,4 \tag{10}$$

The supply flow rate Q_s and load flow rate Q_L are calculated by the nonlinear equations (11) and (12)[18], where the C_d is the flow discharge coefficient, A_1 and A_2 are open areas of the orifices of the valve, P_s and P_L are the pressure of supply flow and the pressure drop across the load, and ρ is the density of the fluid.

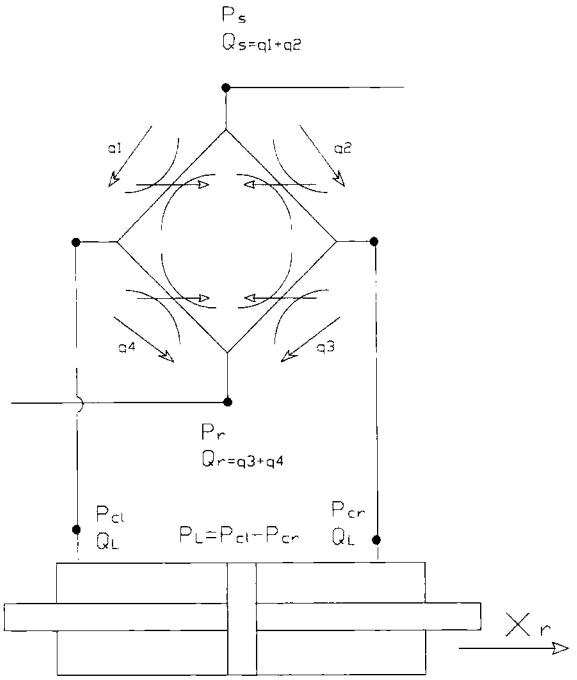

Fig. 5 Schematic of rotary spool valve and hydraulic cylinder

$$\begin{cases} Q_s = C_d A_1 \sqrt{\dfrac{1}{\rho}(P_s - P_L)} + C_d A_2 \sqrt{\dfrac{1}{\rho}(P_s + P_L)} & (11) \\ Q_L = C_d A_1 \sqrt{\dfrac{1}{\rho}(P_s - P_L)} - C_d A_2 \sqrt{\dfrac{1}{\rho}(P_s + P_L)} & (12) \\ \dot{P}_L = \dfrac{2\beta(Q_L - A_P \dot{x}_P)}{V_{half}} & (13) \end{cases}$$

As the same as the steering oil in the supply line, the oil in the chamber of hydraulic cylinder is also considered as compressible fluid. Equation (13) is the governing equation for pressure building up, $\dot{P}_L$, in the chamber. In the equation, A_P is the area of piston, $\dot{x}_P$ is the velocity of piston, V_{half} is the half volume of the chamber and β is the bulk modulus of the oil.

In the study of hydraulic power steering systems, A_1 and A_2 in Eqs. (11) and (12) need special attention. Unlike normal lateral spool valves and rotary spool valves, the valves used in steering systems have more complicated orifice shapes. The reason is that the valves with simple shape orifices will suddenly shut the outlets, and as a result this kind of valve could not satisfy the requirement of the vehicle steering feeling and may induce steering system vibration. Hence the edges of rotary spool slots used in steering systems are designed and manufactured with primary and secondary edges to obtain suitable hydraulic boost characteristics. Figure 6 is a top view schematic of the open area. When the spool rotates related to the sleeve, one side of orifice is opened and the other side is closed.

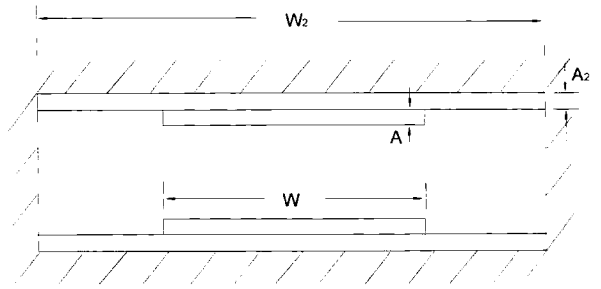

Fig. 6 Schematic of open area of spool valve

At first, the width of A_2 of the long open edge, W_2, decreases, and after a certain angular displacement is turned, the W_2 closes totally and the short open edge, W, becomes the only open area. It is evident that the closing area of the orifice is nonlinear against the relative rotational degree between spool and sleeve.

Equation (14) shows the nonlinearity of the closing area, where R is the radius of spool, φ is the rotational degree, and φ_{key} is the certain degree which makes the long open edge closed.

$$\text{Closing Area} = \begin{cases} AW + (A_2 - R\varphi)W_2 & \text{if } \varphi \le \varphi_{key} \\ (A + A_2 - R\varphi)W & \text{if } \varphi > \varphi_{key} \end{cases} \tag{14}$$

Using small computing steps, numerical calculation is conducted to solve Eqs. (11) to (14) which include nonlinear components and the "stiff" hydraulic elements.

5. Free Vibration Analysis

The integrated power steering system is linearized and its free vibration analysis is performed to investigate the natural frequencies and mode shapes of the mechanism subsystem.

Figure 7 shows one of the system's natural frequencies and its mode shapes when the pinion is at the center position of the rack. In the figure, the 12 points represent the 12 elements of mechanism and the lengths of the vertical lines on the 12 points show the normalized modal coefficients at the selected natural frequency of 7.18 Hz. The symbol θ represents the angular displacement and x represents the linear displacement and they are corresponding to Fig. 2 and Eq. (1).

It can be noticed in Fig. 7, the values of mode shapes of the steering wheel and steering column are the largest, and the value of pinion's mode shape is also considerable. Because of this, the steering wheel, steering column and pinion are the main vibration components, or called dominant components, at this natural frequency (7.18 Hz), and they affect this natural frequency much greater than other components do.

The 12 DOF steering system has 12 natural frequencies, and the variable ratio of rack and pinion gear affects all of the natural frequencies. The 7.18 Hz and 87.07 Hz

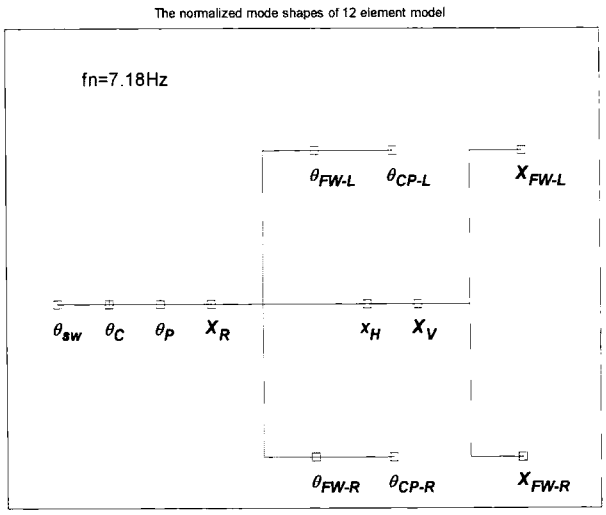

Fig. 7 Natural frequency at 7.18 Hz and mode shapes

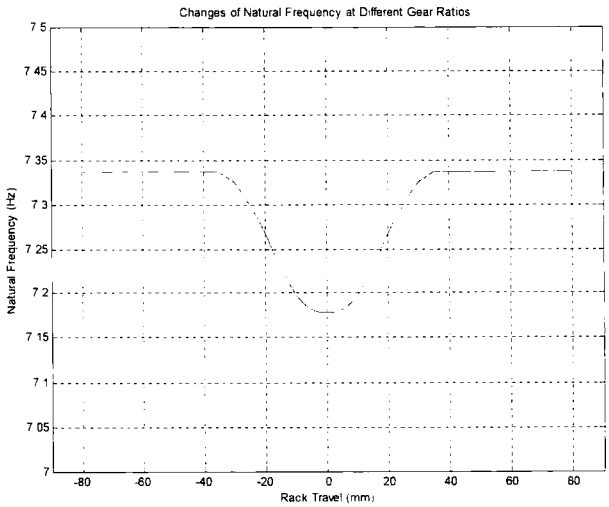

Fig. 8 Changes of natural frequency about 7.18 Hz at different gear ratios

frequencies are analysed as examples to illustrate the effects of ratio on the natural frequencies of the system. A relationship between the displacement of the rack and the natural frequency is shown in Fig. 8. When the pinion is at the center position of the rack, the rack gain is at the maximum value (refer to Fig. 1) and the natural frequency of the mode shown in Fig. 7 (7.18 Hz) is the lowest. When the pinion approaches to the two ends of the rack, the rack gain decreases and then keeps constant and the frequency increases until reaches a constant value (7.34 Hz). From the center of the rack to the end of it, the natural frequency increases about 2.2%. Figure 9 shows the natural frequency at 87.07 Hz and its mode shapes of the system. Same as Fig. 7, this frequency (87.07 Hz) also occurs when the pinion is at the center position of the rack. The values of mode shapes of the steering column and pinion are the largest ones, and the value of steering wheel mode shape is small but still larger than other 9 elements.

The effects of the variable ratio on the natural freqency about (87.07 Hz) is shown in Fig. 10. In contrast to Fig. 8, the natural frequency of the mode shown in Fig. 10 is the highest one (87.07 Hz) when the pinion is at the center position of the rack. When the pinion approaches to the two ends of the rack, the frequency decreases until reaches a constant value (82.31 Hz). The 5.5% decrease shows the varaible ratio affects this frequency (about 87.07 Hz) more than the previous one (about 7.18 Hz). In addition, it is found that the variable ratio does not affect the linearized mode shapes much.

6. Transient Vibration Analysis

Three subsystems, including the mechanism, supply line and rotary spool valve, as discussed in the previous sections, are integrated into a highly nonlinear hydraulic power steering system model. Runge-Kutta method is used in the numerical simulation to analyze the forced response of the steering system in time domain. Steering at zero vehicle speed is demonstrated here as an example because the highest hydraulic force is required in this situation and steering shudder is most likely to occur.

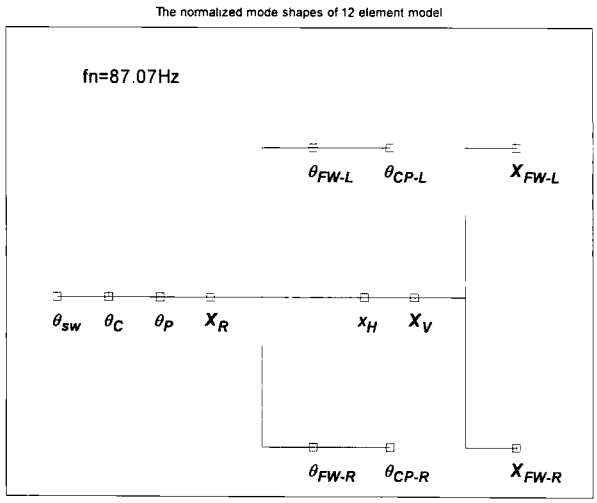

Fig. 9 Natural frequency at 87.07 Hz and mode shapes

Figures 11 and 12 show the simulated responses of a constant ratio (CR) steering system and a variable ratio steering system (VR) respectively. The input of the two steering systems is same. At time 0, the power steering system is in neutral, then from time 0 a constant angular velocity input (1 rad/s) is applied on the steering wheel. In Figs. 11 and 12 (also in Figs. 17 and 18), the top left plot is the angular displacement of the steering wheel and the pinion, the top right plot shows the angular displacement of the front wheels and contact patches, the bottom left plot shows the twist angle of the torsional bar and the boost force in the hydraulic chamber is shown in the bottom right plot.

It is found that the angular displacement of front wheels of the VR steering system is almost the same as the displacement of the CR steering system after 1 second, but it is greater than the latter one after 2 seconds. The reason is that the gear ratios of the two systems are not much different when the pinion rotates in the central area of the rack, but the ratio of VR system decreases sharply when the pinion meshes the side part of the rack while the ratio of CR system is still as same as the beginning. It clearly shows the variable ratio system can reduce the lock-to-lock circles of the steering wheel. In the bottom right plots of Figs. 11 and 12, the boost force of the hydraulic power cylinder starts to oscillate after 0.2 second. The reason is, before 0.2 second the wheels and contact patches of tyres do not move due to the friction forces of the system, especially the friction between the tyres and ground. After 0.2 second, the sum of the force applied on the rack from the pinion and the boost force of hydraulic

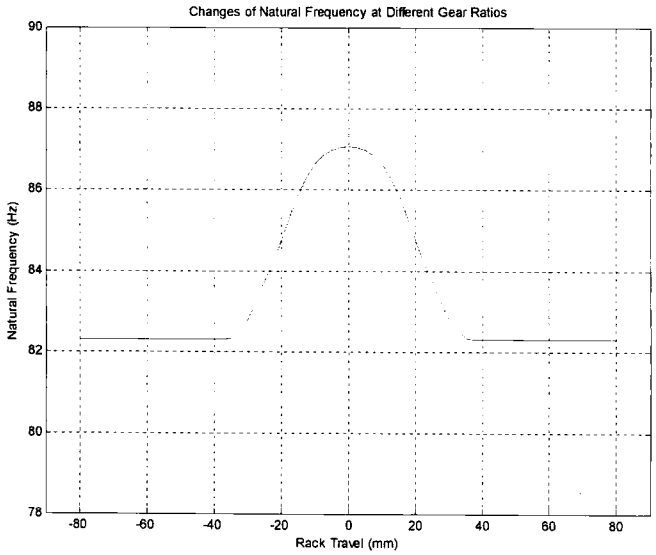

Fig. 10 Changes of natural frequency about 87.07 Hz at different gear ratios

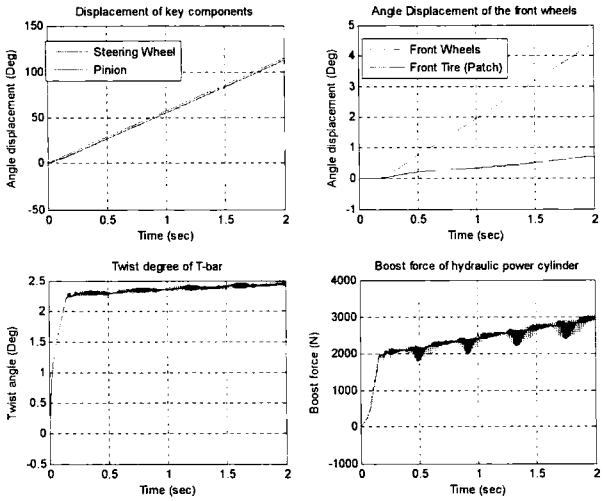

Fig. 11 Response of constant ratio gear hydraulic power steering system

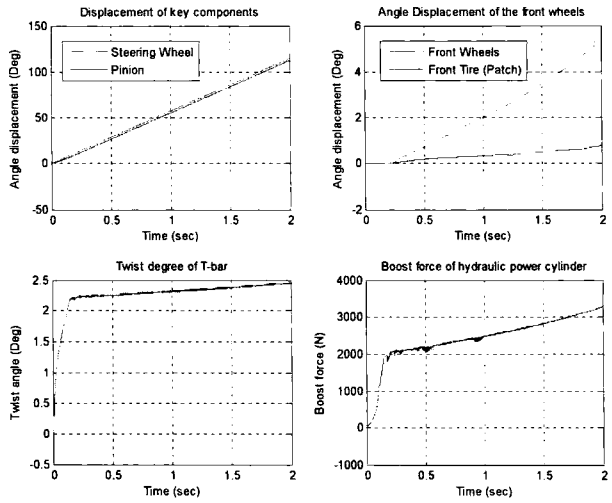

Fig. 12 Response of variable ratio gear hydraulic power steering system

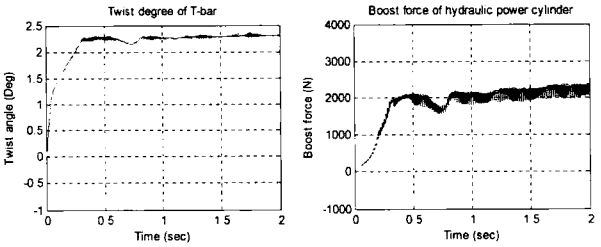

Fig. 13 Response of CR system

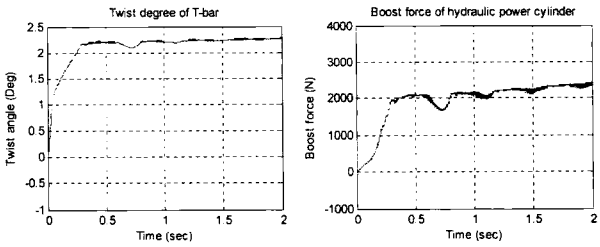

Fig. 14 Response of VR system

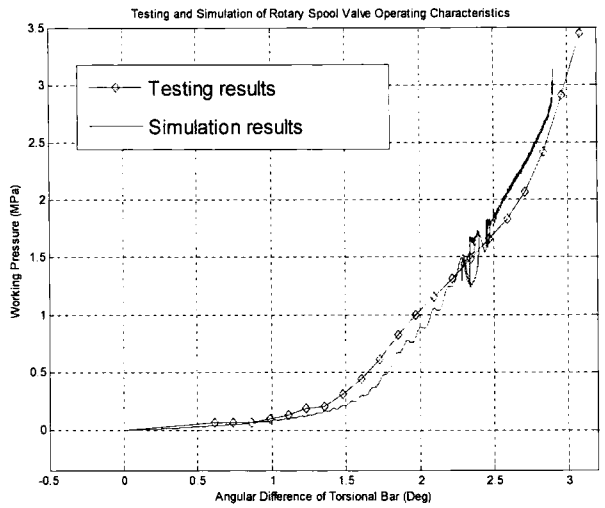

Fig. 15 Simulation and testing results of characteristics of rotary spool valve

cylinder is greater than the friction forces, and the movement of wheels and tyres induce the vibration of the system. Although the vibration is small, the oscillation of the boost force is considerable because the highly nonlinear characteristics of the rotary spool valve. The amplitude of boost force oscillation in VR system is less than the amplitude in CR system. It shows the VR steering system has better dynamic performance than the CR system. Respectively, Figs. 13 and 14 show the responses of a CR system and a VR system due to a relatively slow constant angular velocity input (0.5 rad/s) applied on steering wheel. It simulates the driver slowly turns the steering wheel at a small space (say, parking lot). It can be seen that the oscillation is greater that the situations shown in Figs. 11 and 12 because the vibration of the tyres affects the system more, and the VR system is still better than CR system.

The rotary spool valve is the key component of the hydraulic power steering system, and its operating characteristics have significant influences on the performance of the whole steering system. Figure 15 shows the testing results and simulation results of the characteristics of the rotary spool valve which is presented by the relationship between the twist angle of the torsional bar and the working pressure of the hydraulic cylinder. The test records the steady state of the working pressures at discrete twist angles of the torsional bar. The simulated result which is produced from the mathematic model well agrees with the testing result. Moreover, the vibration in the simulated result captures the dynamic relationship between the twist angle and the pressure which is mainly caused by the compressibility of working fluid and the elasticity of supply line during the steering process.

Besides the constant angular speed input, a ramp torque input, shown in Fig. 16, is used in the simulation of the CR and VR steering system. The ramp torque input

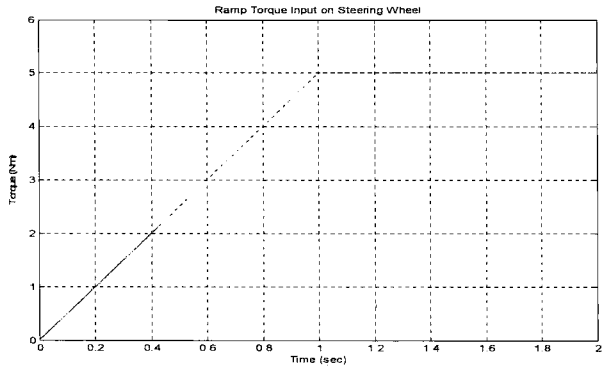

Fig. 16 Ramp torque input applied on steering wheel

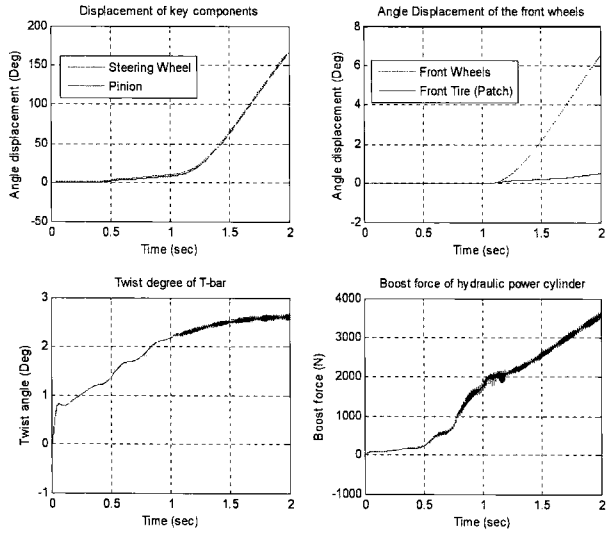

Fig. 17 Response of constant ratio gear hydraulic power steering system

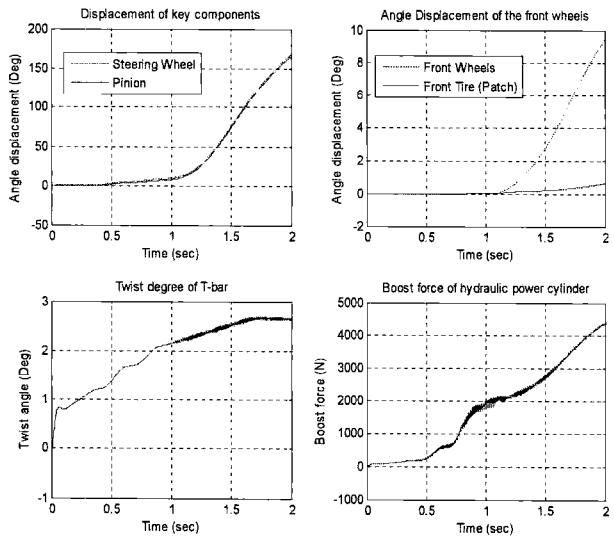

Fig. 18 Response of variable ratio gear hydraulic power steering system

simulates the driver gradually increase the torque on the steering wheel from 0 Nm to 5 Nm at the first second and then keep inputting 5 Nm torque after that.

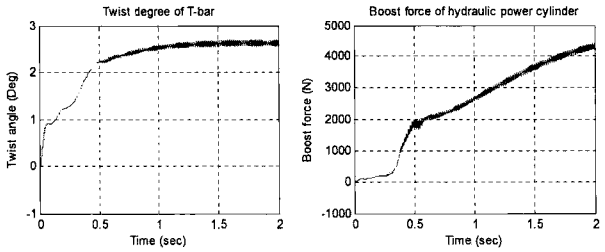

Fig. 19 Response of CR system

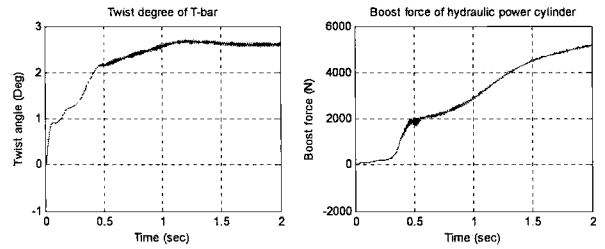

Fig. 20 Response of VR system

Figures 17 and 18 respectively show the different responses of the CR steering system and the VR steering system. Similar to Figs. 11 and 12, VR system obtains greater angular displacement of front wheels and tyres than CR system during a same time range, and the vibration of VR system is less severe than that of the CR system. A quicker ramp input is also conducted and the responses of the CR and VR systems are shown in Figs. 19 and 20. This input simulates a steering wheel torque rapidly increasing from 0 Nm to 5 Nm within 0.2 second. Again, the VR system has better performance than CR system.

7. Conclusions

A highly nonlinear hydraulic power steering system model has been developed and its free and forced vibration analysis have been performed. The mechanism subsystem, hydraulic supply line subsystem and the rotary spool valve subsystem are modeled in detail and then integrated into the completed system model kinetically. The numerical simulations have been conducted to investigate the dynamics of the nonlinear parametric steering system. The hydraulic power steering system equipped variable ratio rack and pinion gear behaviors significantly differently from its constant ratio counterpart does. It is found that the variable ratio of the rack and pinion gear significantly affects not only the system natural frequencies but also reduces the vibration under angular dispalcement with a constant rate and ramp torque steering inputs. The developed analytical VR hydraulic power steering model produces valid predictions of the system's behavior and therefore could assist engineers in the design and analysis of the complete systems.

Appendix: Stiffness Matrix of Variable Ratio Rank and Pinion Gear Steering System

$$
\begin{bmatrix}
K_C & -K_C & 0 & 0 & 0 & 0 & 0 & 0 & 0 & 0 & 0 & 0 \\
-K_C & K_C+K_B & -K_B & 0 & 0 & 0 & 0 & 0 & 0 & 0 & 0 & 0 \\
0 & -K_B & K_B+K_P & 0 & -\frac{K_P}{N} & 0 & 0 & 0 & 0 & 0 & 0 & 0 \\
0 & 0 & 0 & K_V & 0 & 0 & 0 & 0 & 0 & 0 & 0 & -K_V \\
0 & 0 & -\frac{K_P}{N} & 0 & \frac{K_P}{N^2}+K_{TR-L}+K_{TR-R} & -l\cdot K_{TR-L} & -l\cdot K_{TR-R} & 0 & 0 & 0 & 0 & 0 \\
0 & 0 & 0 & 0 & -l\cdot K_{TR-L} & l^2\cdot K_{TR-L}+K_{T-RO} & 0 & -K_{T-RO} & 0 & 0 & 0 & 0 \\
0 & 0 & 0 & 0 & -l\cdot K_{TR-R} & 0 & l^2\cdot K_{TR-R}+K_{T-RO} & 0 & -K_{T-RO} & 0 & 0 & 0 \\
0 & 0 & 0 & 0 & 0 & -K_{T-RO} & 0 & K_{T-RO} & 0 & 0 & 0 & 0 \\
0 & 0 & 0 & 0 & 0 & 0 & -K_{T-RO} & 0 & K_{T-RO} & 0 & 0 & 0 \\
0 & 0 & 0 & 0 & 0 & 0 & 0 & 0 & 0 & K_{S-L}+K_{T-LA} & 0 & -K_{S-L} \\
0 & 0 & 0 & 0 & 0 & 0 & 0 & 0 & 0 & 0 & K_{S-R}+K_{T-LA} & -K_{S-R} \\
0 & 0 & 0 & -K_V & 0 & 0 & 0 & 0 & 0 & -K_{S-L} & -K_{S-R} & K_{S-L}+K_{S-R}+K_V
\end{bmatrix}
$$

References

(1) Wang, T., Hydraulic Power Steering System Design and Optimization Simulation, SAE Technical Paper Series 2001-01-0479, (2001).

(2) Lozia, Z. and Zardecki, D., Vehicle Dynamics Simulation with Inclusion of Freeplay and Dry Friction in Steering System, SAE Technical Paper Series 2002-01-0619, (2002).

(3) Taheri, S., Kazemi, R. and Tabatabai, M., Analysis and Optimization of Vehicle Steering System, SAE Technical Paper Series 981113, (1998).

(4) Vijayakumar, S. and Barak, P., Application of Bond Graph Technique and Computer Simulation to the Design of Passenger Car Steering System, SAE Technical Paper Series 2002-01-0617, (2002).

(5) Sharp, R.S. and Granger, R., On Car Steering Torque at Parking Speed, Proceedings of the Institution of Mechanical Engineers, Vol.217, Part D: Journal of Automobile Engineering, (2003), pp.87–96.

(6) Ferries, G.R. and Arbanas, R.L., Control/Structure Interaction in Hydraulic Power Steering Systems, Proceedings of the American Control Conference Albuquerque, New Mexico, USA, (1997), pp.1146–1151.

(7) Matsunaga, T., Tanaka, T. and Nishimura, S., Analysis of Self-Excited Vibration in Hydraulic Power Steering System: Prevention against Vibration by Supply Line, SAE Technical Paper Series 2001-01-0488, (2001).

(8) Qatu, M., Llewellyn, D. and Edwards, R., Correlation of Hydraulic Circuit Dynamic Simulation and Vehicle, SAE Technical Paper Series 2000-01-0811, (2000).

(9) Qatu, M.S., Llewellyn, D.R. and Spadafora, W.G., Measurement of Steering Gear Impedance, Experimental Mechanics, Vol.41, No.2 (2001), pp.151–156.

(10) Smid, G.E., Qatu, M.S. and Drew, J., Optimizing the Power Steering Components to Attenuate Noise and Vibrations, European Conference on Vehicle Noise and Vibration, IMechE Headquarters, London, UK, (1998), pp.103–112.

(11) Phillips, R.W., Self-Excited Vibration in Hydraulic Steering Racks, SAE Technical Paper Series 2003-01-0580, (2003).

(12) Neureder, U., Investigation into Steering Wheel Nibble, Proceedings of the Institution of Mechanical Engineers, Vol.216, Part D: Journal of Automobile Engineering, (2002), pp.267–277.

(13) Takeuchi, S. and Adachi, E., Analysis and Reduction of Power Steering Noise during Static Steering Operation, SAE Technical Paper Series 950581, (1995).

(14) Post, J.W., Modeling, Simulation and Testing of Automobile Power Steering Systems for the Evaluation of on-Center Handling, Ph.D. Dissertation, Clemson University, Clemson, South Carolina, (1995).

(15) Heathershaw, A., Optimizing Variable Ratio Steering for Improved on-Centre Sensitivity and Cornering Control, SAE Technical Paper Series 2000-01-0821, (2000).

(16) Heathershaw, A., Matching of Chassis and Variable Ratio Steering Characteristics to Improve High Speed Stability, SAE Technical Paper Series 2004-01-1103, (2004).

(17) McCloy, D. and Martin, H.R., Control of Fluid Power: Analysis and Design, 2nd (Revised) Edition, (1980), pp.236–240, Ellis Horwood Limited, Chichester, England.

(18) Merritt, H.E., Hydraulic Control Systems, (1967), John Wiley & Sons, New York, NY.

(19) Wang, M., Zhang, N. and Misra, A., Sensitivity of Key Parameters to Dynamics of Hydraulic Power Steering Systems, Submitted to the SAE 2005 Noise and Vibration Conference to Be Held in Traverse City, MI, USA, (2005).